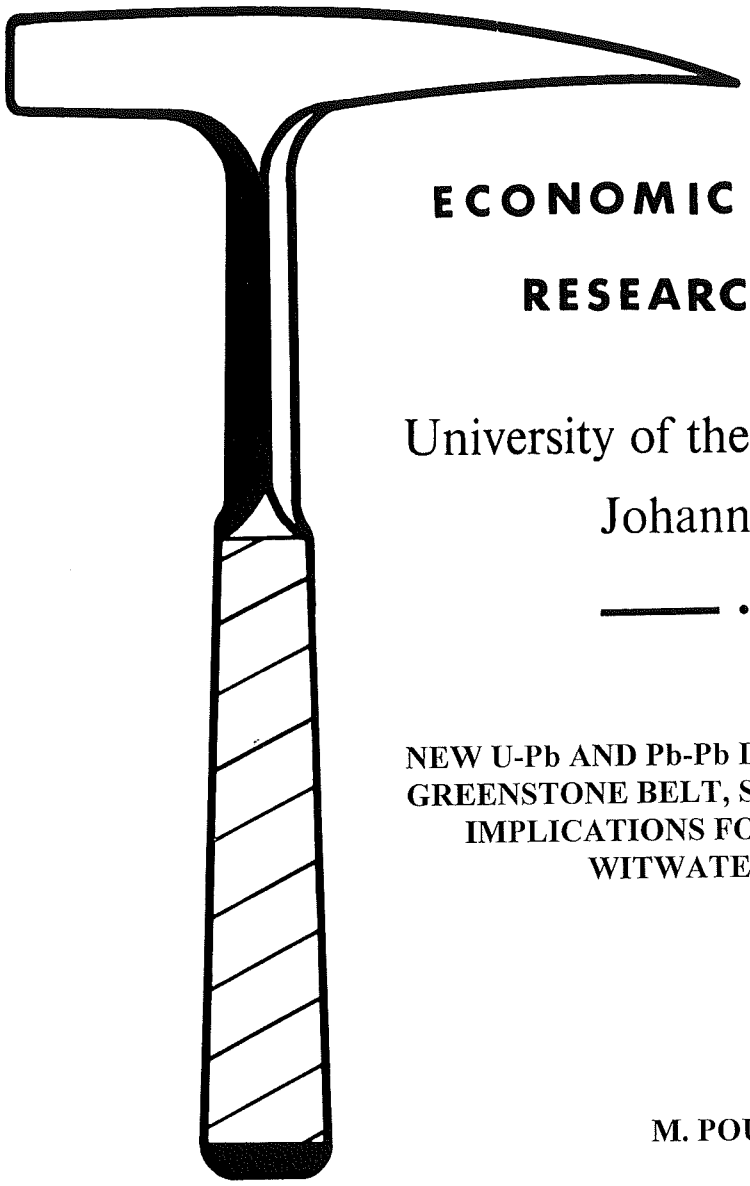

ECONOMIC GEOLOGY

RESEARCH UNIT

University of the Witwatersrand

Johannesburg

NEW U-Pb AND Pb-Pb DATA ON THE MURCHISON GREENSTONE BELT, SOUTH AFRICA AND THEIR IMPLICATIONS FOR THE ORIGIN OF THE WITWATERSRAND BASIN

M. POUJOL, J.P. RESPAUT, L.J. ROBB
and C.R.ANHAEUSSER

INFORMATION CIRCULAR No. 319

UNIVERSITY OF THE WITWATERSRAND
JOHANNESBURG

NEW U-Pb AND Pb-Pb DATA ON THE MURCHISON GREENSTONE BELT, SOUTH AFRICA AND THEIR IMPLICATIONS FOR THE ORIGIN OF THE WITWATERSRAND BASIN

by

M. POUJOL[1], J.P RESPAUT[1], L.J. ROBB[2] and C.R. ANHAEUSSER[2]
([1] UMR 5567 CNRS/UM2, ISTEEM, cc066, Université Montpellier II,
34 095 Montpellier Cedex 5, France
[2]Department of Geology-Economic Geology Research Unit,
University of the Witwatersrand, P/Bag 3, WITS 2050, South Africa)

ECONOMIC GEOLOGY RESEARCH UNIT
INFORMATION CIRCULAR No. 319

December, 1997

NEW U-Pb AND Pb-Pb DATA ON THE MURCHISON GREENSTONE BELT, SOUTH AFRICA AND THEIR IMPLICATIONS FOR THE ORIGIN OF THE WITWATERSRAND BASIN

ABSTRACT

The 3.09-2.97 Ga Murchison greenstone belt represents one of a number of Archaean volcano-sedimentary belts within the Archaean Kaapvaal Craton of South Africa and constitutes one of the world's largest antimony producing areas. The Murchison greenstone belt also hosts gold, mainly associated with antimony mineralization, as well as volcanogenic massive sulfide copper-zinc mineralization and emeralds. The present study presents new U-Pb data that was obtained to determine the timing of mineralization and also assess the potential role that granitoids have played in the ore-forming processes. Techniques utilized include systematic U-Pb isotope determinations on single zircon grains from intrusions, as well as the direct dating and characterization of mineralization by Pb-Pb isotopic determinations of pyrite. Three main magmatic events are identified at ca. 2.97, 2.82 and 2.68 Ga for the Maranda batholith (which intrudes the Antimony Line structure), the Willie and the Mashishimala Granites respectively. Pyrites associated with both Sb-Au and Cu-Zn mineralization define a secondary isochron with a reasonably well constrained age of 2.97 Ga which suggests that they are spatially and genetically associated with the 2.97 Ga Maranda Batholith and the rhyo-dacitic Rubbervale Formation. Thus, VMS style copper-zinc mineralization is syngenetic with respect to the Rubbervale Formation, whereas Sb-Au lode mineralization along the Antimony Line structure appears to be related to magmatic fluid egress from the Maranda batholith. Pb-Pb isotopic signatures of pyrite associated with emerald mineralization along the southern flank of the belt reflects mixing between Pb derived from the older gneissic basement and that characteristic of the major magmatic event at 2.97 Ga. The 2.97 Ga Maranda batholith and Rubbervale Formation, therefore, represents a highly prospective metallotect that are relevant, not only to exploration in the Murchison region itself, but to the important question of the source of Witwatersrand gold.

__oOo__

NEW U-Pb AND Pb-Pb DATA ON THE MURCHISON GREENSTONE BELT, SOUTH AFRICA AND THEIR IMPLICATIONS FOR THE ORIGIN OF THE WITWATERSRAND BASIN

CONTENTS

____oOo____

Published by the Economic Geology Research Unit
Department of Geology
University of the Witwatersrand
1 Jan Smuts Avenue
Johannesburg 2001
South Africa

ISBN 1-86838-196-X

GEOLOGICAL SETTING

The east-northeast-trending Murchison greenstone belt (MGB), also referred to as the Murchison schist belt (Hall, 1912; Vearncombe et al., 1992), takes the form of isoclinally folded, narrow (generally less than 20km wide), elongated sequences of deformed metavolcanic and metasedimentary rocks intruded by a variety of Archaean granites and orthogneisses (Fig. 1). Extensive fragmentation of the belt has taken place to the east and southwest where numerous large greenstone xenoliths occur in compositionally and chronologically diverse granitoids (Hall 1912; Van Eeden et al., 1939; Minnitt and Anhaeusser, 1992; Vearncombe et al., 1992).

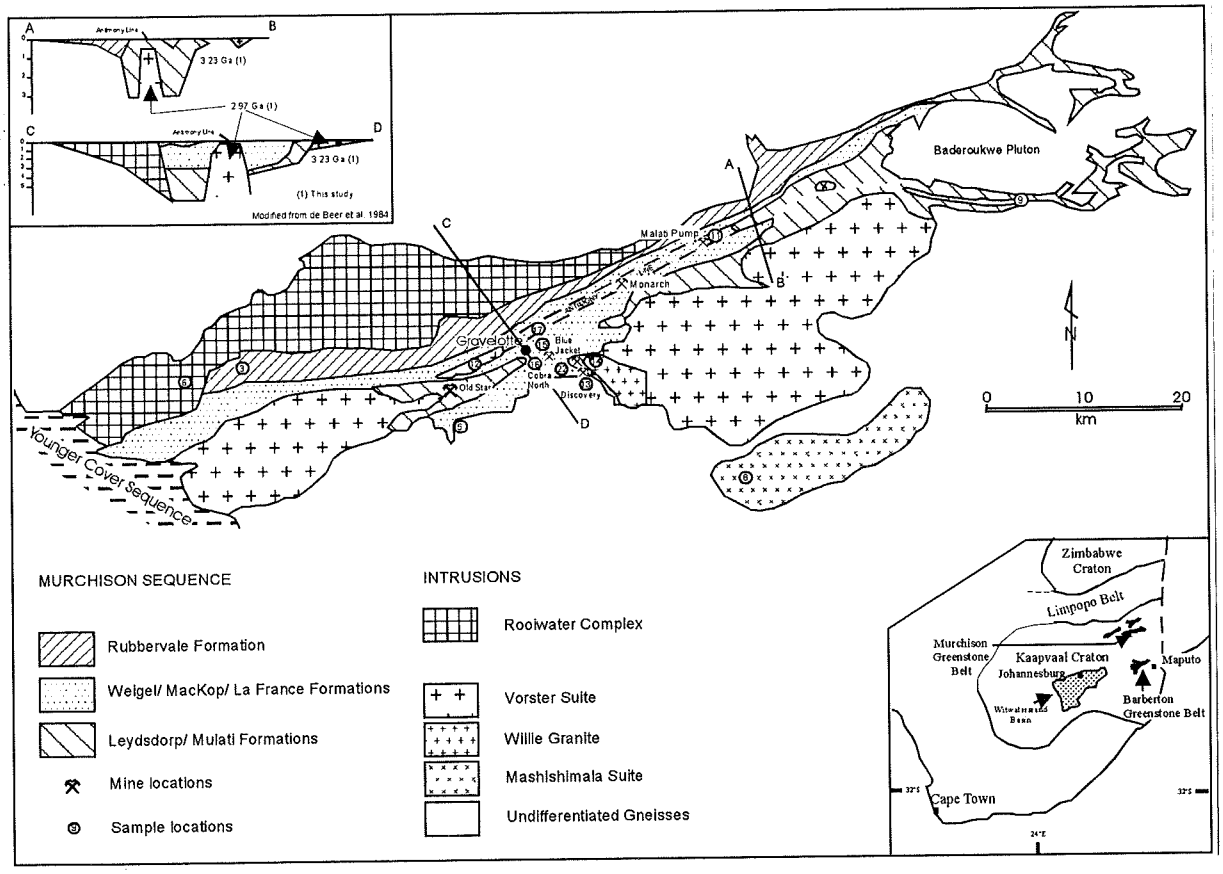

Figure 1 : Simplified geological map of the Murchison belt showing the location of the samples. Inset map shows the MGB in relation to other belts on the craton. Profiles AB and BC show localities of geophysical models (second inset).

Due to the intensity of deformation and the absence of definitive field relationships, controversy exists as to the stratigraphic order in the belt. Viljoen et al. (1978) and Anhaeusser and Wilson (1981) recognized lithological similarities with the Barberton greenstone belt (BGB) and advocated an essentially north-younging sequence of mafic and ultramafic komatiitic and high-magnesian metavolcanics, talcose and serpentinitic rocks occupying both the southern flank of the belt as well as the numerous xenoliths in the neighbouring granites (Mulati and Leydsdorp Formations - SACS 1980).

Mafic-to-felsic volcanics and volcanoclastic sediments comprising pillowed metabasalts, amphibole-chlorite schists, chlorite-sericite schists, quartz-sericite schists, quartz porphyries, as well as the Antimony Line, occupy the central portion of the belt (La France and Weigel Formations - S.A.C.S. 1980). Quartzites, conglomerates and quartz-sericite-chlorite schists (MacKop Formation) occur south of the Baderoukwe gneiss pluton (Fig. 1) in the Bawa Schist Belt (SACS, 1980; Minnitt

and Anhaeusser, 1992). Intensely sheared intermediate-to-felsic lavas, pyroclastic rocks, quartz-feldspar porphyries and the mineralized "Copper-Zinc Line" constitute the Rubbervale Formation which occurs along the northern flank of the MGB. The Rooiwater Complex, also on the northern side of the MGB lacks pervasive deformation and is a metamorphosed layered complex younging to the south (Van Eeden et al., 1939; SACS, 1980; Vearncombe et al., 1992).

A suite of potassic granitoids rocks (Vorster suite; Fig.1) intrudes the southern margin of the MGB, but are generally poorly exposed such that no clear field evidence exists to establish their mutual relationships. The granitoids range in composition between granodiorite and alkali-feldspar granite suggesting that all these units might be genetically related and could form a single batholith encompassing or underlying the MGB (Fig.1, inset) (De Beer, 1982; De Beer, et al. 1984, Vearncombe et al., 1992). Migmatites and orthogneisses of more sodic compositions (tonalite-trondhjemite-granodiorite) occur both to the north (Goudplaats) and south (Makhutswi) of the MGB. The final magmatic event in this region is represented by the post-tectonic Mashishimala granite pluton (Fig. 1), whose age is discussed below.

CHARACTERITICS OF THE MINERALIZATION

There are several styles of mineralization in the MGB; gold, antimony, arsenic, tungsten and mercury are the most frequent associations found in hydrothermal mineralized systems of the Antimony Line of the MGB (Viljoen et al., 1978; Vearncombe, 1992; Vearncombe et al., 1992). In addition, copper-zinc mineralization in the Rubbervale Formation is believed to bear similarities with volcanogenic massive sulphides systems (Taylor, 1981; Terblanche and Lewis, 1995), whereas emerald mineralization is associated with the intrusion of small felsic bodies and pegmatites into mafic schists (Robb and Robb, 1985). Finally, magmatic segregations of titaniferous magnetite seams are associated with igneous differentiation in the Rooiwater Complex (Reynolds, 1986).

Gold mineralization

Gold has been mined in the past from a total of 59 mines, most of which have now been worked out. Deposits are described as mesothermal lode gold types, although an origin related to gold-enriched emanations deriving from volatile phases linked to intrusive granites has also been suggested (Kedda et al. 1990; Kedda, 1992). The model established for gold deposits of the BGB has been applied to the MGB (Saager and Köppel, 1976) with a classification into two groups : (i) massive stratabound replacement sulphide deposits like those at Gravelotte, Monarch and United Jack, or exhalative sedimentary types, such as Letaba; and (ii) gold-rich quartz veins such as the Old Star Mine. For the second type, gold and related elements are thought to be derived mainly from the surrounding rocks by remobilization processes during metamorphism (Viljoen et al. 1969, 1970; Saager 1973, 1974). These authors suggested that intrusive granites had played an important role in the mineralization, but that they could not be considered as the ultimate source of the gold.

Recently, Vearncombe et al. (1992) classified the gold mineralization into six different types; (i) mineralization associated with stibnite and berthierite in carbonaceous rocks; (ii) associated with arsenopyrite and pyrite in ferruginous cherts and BIF; (iii) disseminated sulphides in chlorite schists; (iv) auriferous pyrite and other sulphides in shear zones, (v) quartz veins spatially related to shear zones; and (vi) zones with minor quartz veining and disseminated pyrite.

Kedda (1992) was particularly interested in gold mineralization associated with albitised felsic intrusions (type vi in Vearncombe's classification). The albitites are associated with numerous intrusions along major structural discontinuities of the MGB, and are thought to have originated during sodic metasomatism (albitisation) related to deuteric and post-magmatic fluids. This type of mineralization is characterised by an atypical Mo-W-Be-Sb-Au-B-Hg paragenesis associated with a

mesothermal temperature regime. Stable isotopes, as well as fluid inclusions, suggest an intimate relationship between Au-Sb and the granites as well as a fluid homogeneity on a regional scale with local scale phase separation (Kedda, 1992; Kedda et al., 1990).

Antimony mineralization

The economic importance of antimony increased during and after the Second World War. As a result, the production of antimony from the Consolided Murchison mines reached 25 000 tons (15000 tons metal) in 1951 and by 1986, the total antimony production of the MGB represented 18% of global production.

Antimony mineralization is essentially in the form of stibnite and berthierite ($FeSb_2S_4$) associated with pyrite and arsenopyrite. Mineralization is hosted along the 35km long, 250m wide, Antimony Line, which represents a major shear zone (Vearncombe et al., 1988). A total of eighteen mines have been worked in this area which represents one of the major antimony producing regions of the world. Archaean antimony deposits are a relatively rare phenomenon which implies that this style of mineralization must be characterized by an unusual set of processes. Gold is also commonly associated with the antimony mineralization which suggests that both elements were enriched during the same mineralization processes (Pearton and Viljoen, 1986).

Emeralds

Emerald mineralization is linked to a pegmatite-rich zone along the southern margin of the belt and is associated with beryl, tourmaline, molybdenite, garnet, aquamarine, chrysoberyl and tantalite. The most favorable host rocks for the development of emeralds are biotite schists, as seen at the Gravelotte Emerald Mine. Traditionally, the emeralds are believed to have formed as a result of the interaction between late-stage, beryllium-bearing pegmatitic granitoids and ultramafic schists (komatiites) of the Mulati Formation (Robb and Robb, 1986). Grundmann and Morteani (1989), however, suggested that the emeralds grew syn-tectonically, during an event of regional metamorphism that may have post-dated the formation of the MGB, and represent porphyroblasts forming as a result of metamorphic mineral reactions at the interface between felsic and mafic rock types.

Other deposits

Discovered in 1936, the deposits of the Monarch Cinnabar Mines have provided a total of 150t of mercury metal between 1939 and 1945 (Pearton, 1986). These deposits are not only the main occurrences in South Africa but are also of the rare Archaean mercury deposit type (i.e. 99% of world mercury deposits are Phanerozoic in age). The ore is localized in sheared quartz-carbonate rocks to the north of the Antimony Line, in contact with quartz-muscovite schists.

The massive base metal sulphide mineralization of the so-called Copper-Zinc Line is located within the Rubbervale Formation, along a contact zone between dominantly tuffaceous rhyolites and overlying pelitic metasediments (Terblanche and Lewis, 1995). The mineralization has many of the characteristics of felsic volcanic-hosted massive sulphide (VMS) deposits of syngenetic origin (Taylor, 1981; Terblanche and Lewis, 1995), observed in many Archaean terranes. Mining production began in 1954 at the Letaba Mine (Hausmann, 1959). Deposits are generally small (400 to 1100m long), but very rich, and appear to be closely associated with felsic volcanic vents (Minnitt, 1981).

METHODOLOGY

Single zircon grain analysis

Zircons were separated using a Wilfley table and a Frantz isodynamic separator. Handpicked zircons were washed with ultrapure diluted nitric acid, abraded (Krogh, 1982), weighed on a Cahn micro-balance and then chemically processed to obtain a combined U and Pb solution (Lancelot et al., 1976; Bruguier et al., 1994). An aliquot of the resulting solution was extracted and mixed with a ^{208}Pb-^{235}U spike for determination of Pb and U concentrations; an unspiked aliquot was used for measurement of Pb isotopic compositions. Analysis were carried out on a rhenium filament and the solution was coprecipated with a 0.25N H_3PO_4-silicagel mixture.

Pyrite analysis

Pyrite was extracted from the samples using the techniques described above. The fractions were carefully selected under binocular microscope, washed in acetone and dissolved in a savilex™ beaker with Aqua-Regea and a few drops of HBr. Lead was separated and purified on ion exchange resin (Bio Rad AG 1x8) with 0.5 N HBr and an elution using 6N HCl. Lead and uranium concentrations were determined from a spiked aliquot (^{207}Pb-^{235}U spike). Lead was loaded onto a Re filament with H_3PO_4 and silicagel, whereas uranium was anaysed on a W filament with $TaCl_5$. The isotopic ratios were measured on a VG Sector Mass Spectrometer, corrected by 0.20 ± 0.05‰ for mass fractionation. Data were reduced using PbDat (Ludwig,1993a). Analytical uncertainties are listed at 2σ. Age determinations were processed using Isoplot (Ludwig, 1993b).

AGE DETERMINATIONS

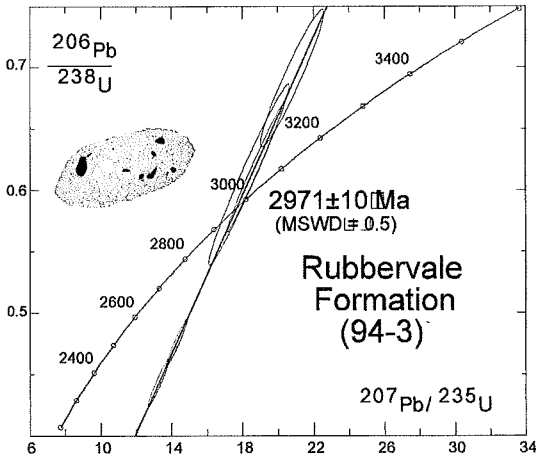

Figure 2 : Concordia diagram sample 94-3.

A sample of rhyolite from the Rubbervale Formation (94-3) was collected along the northern edge of the MGB (Fig. 1). Zircons comprise a homogeneous, euhedral population, generally translucent, pale pink with rare mineral inclusions (Fig. 2, inset). U and Pb contents were typically very low, in the ranges 16-75 and 13-57 ppm respectively (Table 1). The 5 single grains analysed were all reasonably concordant with very similiar $^{207}Pb/^{206}Pb$ ratios (Fig. 2), yielding an upper intercept age of 2,971±10 Ma. This age is considered to reflect the time of crystallization of the acid volcanic rocks of the Rubbervale Formation. The age bis also indistinguishable from a recently published U-Pb zircon date of 2,966.5±1.6 Ma of the Rubbervale Formation (Brandt et al., 1996).

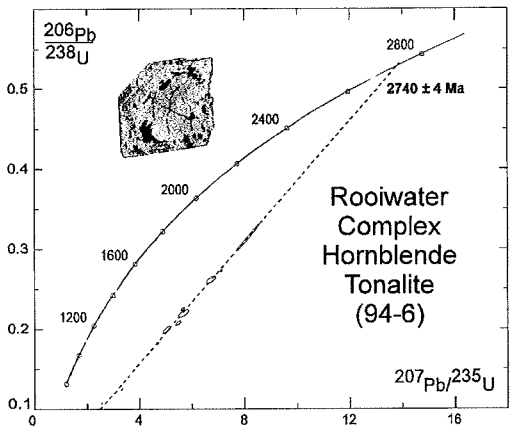

Figure 3 : Concordia diagram sample 94-6.

A sample of hornblende tonalite (94-6) of the Rooiwater Complex yielded abundant prismatic and elongate zircons characterized by zoned alteration, intense fracturing and numerous quartz, xenotime and Al-silicate mineral inclusions (Fig. 3, inset). Isotopic ratios are discordant, but the 10 grains analysed yielded fairly consistent $^{207}Pb/^{206}Pb$ ratios pointing to an upper intercept age of 2,740±4 Ma (Fig. 3). This is regarded as a reasonable (minimum) estimate of the age of crystallization of the Rooiwater Complex, and clearly indicates that it is at least 200 Ma younger than the rhyolites of the Rubbervale Formation.

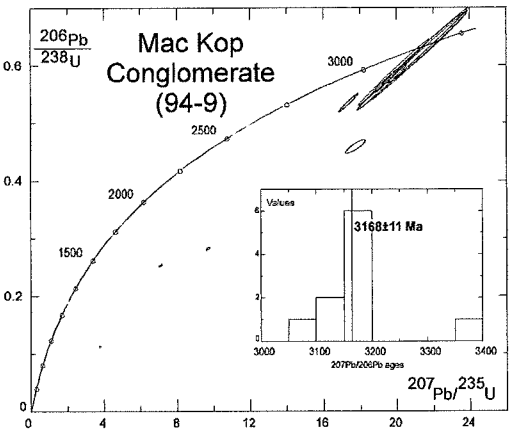

Figure 4 : Concordia diagram sample 94-9.

A sample of metaconglomerate from an arenaceous sequence of cross-bedded and graded quartzites and rudites in the MacKop area of the eastern MGB (94-9) was sampled in order to obtain an indication of the maximum age of sedimentation in the belt. Zircons extracted from this unit were typically subhedral with an absence of well rounded morphologies, suggesting proximal derivation. The data points define a relatively homogeneous population with a mean $^{207}Pb/^{206}Pb$ age of 3,168±11 Ma (Fig. 4). The bulk of the detritus in the sedimentary succession appears to have been derived from the erosion of material of this age and it is pertinent to note that Brandt and Kröner (1993) have identified 3.1 Ga tonalitic gneisses in the vicinity of the MGB. The oldest zircon grain in the sedimentary sequence is discordant but suggests a $^{207}Pb/^{206}Pb$ age of 3,364±18 Ma. The youngest zircon is also slightly discordant and indicates a $^{207}Pb/^{206}Pb$ age of 3,076±4 Ma, which is an estimate for the maximum age of deposition of the MacKop sequence.

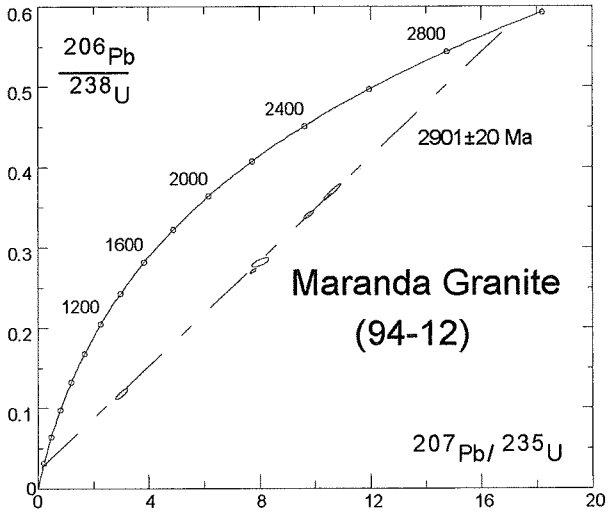

Figure 5 : Concordia diagram sample 94-12.

The granodioritic Maranda intrusion defines the western limit of the Antimony Line in the central portion of the MGB (Fig. 1) and forms part of a murch larger granitoid body that was emplaced along this major tectonic lineament (De Beer et al., 1984; Kedda et al., 1990). The sample (94-12) provided small zircons with variable U and Pb contents, which yielded discordant results but fairly consistent $^{207}Pb/^{206}Pb$ ratios indicating an upper intercept age of 2,901±20 Ma (Fig. 5). This is interpreted as a reasonable (minimum) estimate of the age of emplacement of the Maranda pluton, and also an indication of the upper limit for the age of deformation in the MGB.

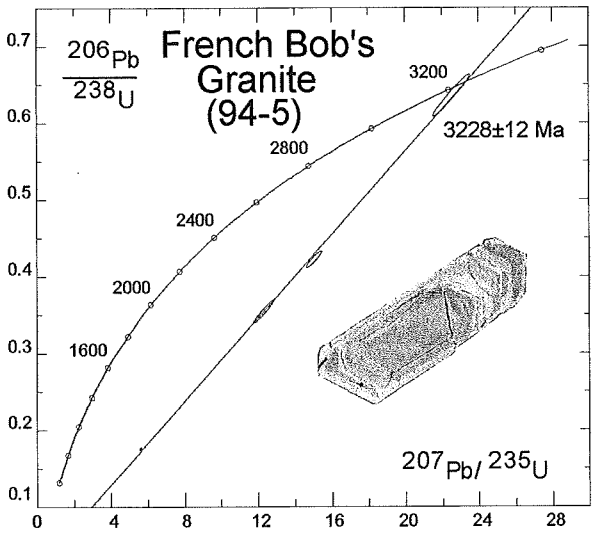

Figure 6 : Concordia diagram sample 94-5.

The sample (94-5) was collected from a TTG gneiss occurring along the southern contact of the MGB at French Bob's gold mine (Fig. 1). Zircons are euhedral, compositionally zoned, highly fractured and contain numerous mineral inclusions, both within the grain and along microfractures (Fig. 6, inset). U and Pb contents in these zircons are fairly low (73-449 and 31-100 ppm respectively) but isotopic ratios are markedly discordant. Four grains were analyzed (Fig. 6) and the most concordant point yields a $^{207}Pb/^{206}Pb$ age of 3,228±12 Ma. This suggests that an older granitoid basement existed in the vicinity of the MGB prior to the formation of the greenstone belt.

This sample was composited from three different locations within the Weigel Formation : 95-17 is a chloritic schist including limonite veins, 95-16 is more felsic in composition and is interpreted as having a volcanoclastic origin and 95-15 is a dark-coloured foliated partially silicified rhyolite. Most of the data plots as concordant to subconcordant points on a concordia diagram (Fig 7), except for 95-16c. The oldest zircon has a $^{207}Pb/^{206}Pb$ age of 3,196±28 Ma, whereas the mean $^{207}Pb/^{206}Pb$ age for the population is 3,087±21 Ma. The latter age can be considered as the best estimate for the emplacement of the Weigel formation volcanics. The heterogeneity of the $^{207}Pb/^{206}Pb$ ages accords with the volcano-sedimentary origin envisaged for the Weigel samples.

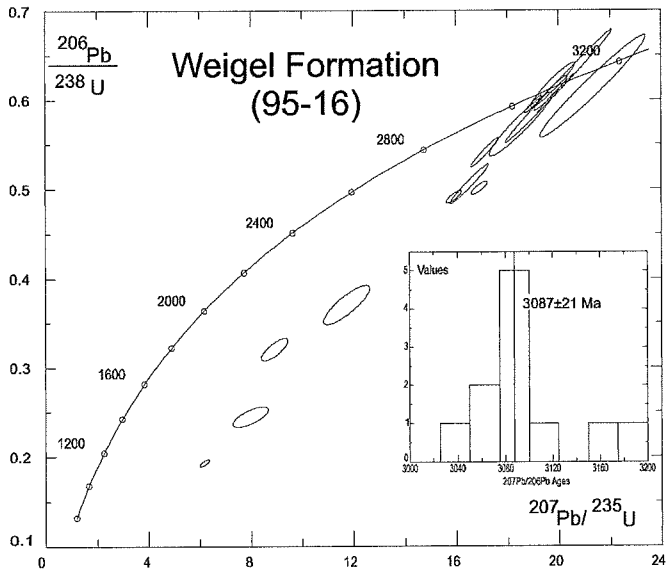

Figure 7 : Concordia diagram samples 95-15, 16 and 17.

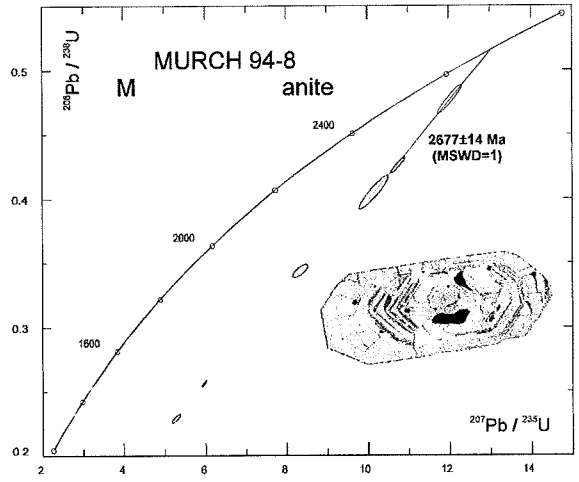

Figure 8 : Concordia diagram sample 94-8.

Sample MURCH 94-8 (Fig. 1) was collected from south of the MGB in the centre of the Mashishimala Suite. According to Vearncombe et al. (1992), this rock is a peraluminous granite. The zircons are generally euhedral, fractured, compositionally zoned and contain numerous inclusions of quartz and alumino-silicates (Fig. 8 inset). Except for the grain Zr GG (Table 1), the U and Pb contents are very similar (160-254 ppm and 65-90 ppm respectively). The upper intercept age calculated from the three least discordant points is 2677 ± 14 Ma (MSWD=1) (Fig. 8). This is considered to reflect the age of the emplacement of the Mashishimala Suite.

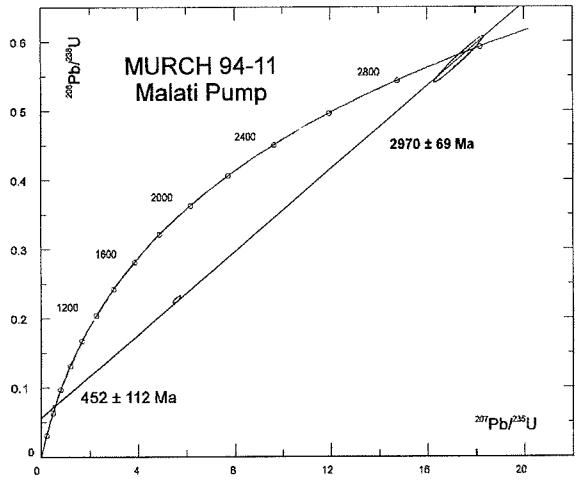

Figure 9 : Concordia diagram sample 94-11.

A granodiorite sample, MURCH 94-11, was collected from the Malati Pump Mine, located on the Antimony Line (Fig. 1). This granodioritic pluton (Kedda et al. 1990) intrudes quartz-chlorite schists and has been itself intruded by a late dolerite dyke. The mineralization at Malati Pump is essentially gold rich with only minor Sb. The sample provided small, translucent zircons with low (Table 1) Pb contents (26-63 ppm) and variable uranium contents (900 to 80 pmm). Four points gave an upper intercept age of 2970 ± 69 Ma with a lower intercept at 452 ± 112 Ma. One of the zircons is perfectly concordant with a $^{207}Pb/^{206}Pb$ age of 2970 ± 15 Ma (Fig. 9). The latter age is considered as the best estimate for the age of the emplacement of the granodiorite. This age is identical, within error, of the Rubbervale Formation (Fig. 2) suggesting that the latter represents the extrusive equivalent of this phase of granite.

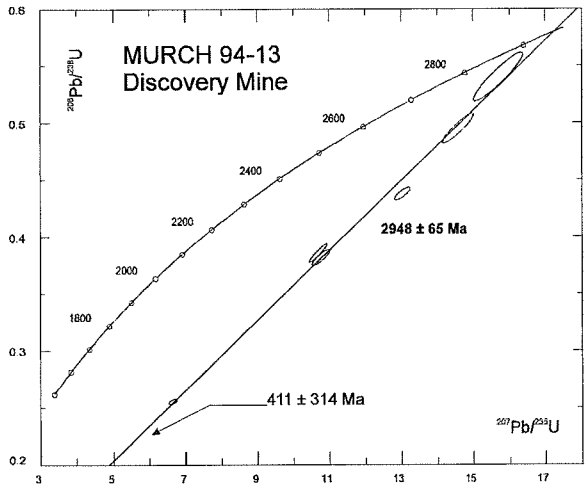

Figure 10 : Concordia diagram sample 94-13.

The Discovery Granite (MURCH 94-13) was sampled close to the Discovery Shaft in the Cobra North portion of the Gravelotte Emerald Mine, along the southern contact of the MGB (Fig. 1). It is similar in appearance to the granodiorites outcropping near Maranda and at the Malati Pump Mine. Zircons are homogeneous, euhedral and translucent. U and Pb contents (Table 1) range respectively between 114-1213 ppm and 66-310 ppm. On a concordia plot (Fig. 10) the data yield an upper intercept age at 2960 ± 43 Ma and a lower intercept at 452 ± 69 Ma.

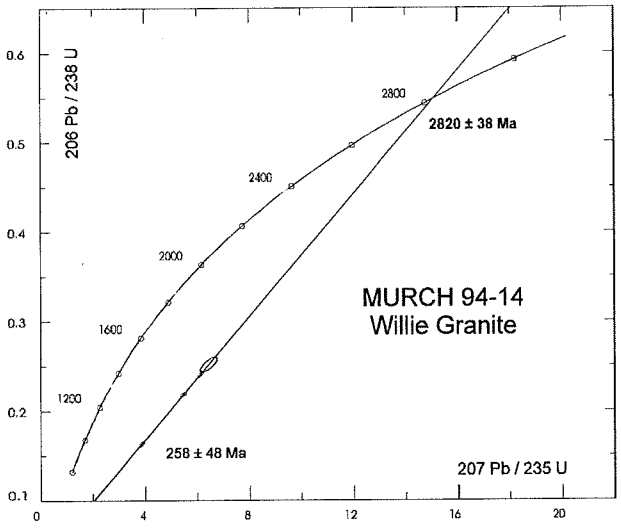

Figure 11 : Concordia diagram sample 94-14

The final sample (MURCH 94-14) is from a biotite-bearing porphyritic granite, the Willie Granite (Fig. 1), which outcrops along the southern flank of the MGB and appears to intrude the Vorster Suite. From a petrographic point of view, the Willie Granite appears to be similar to the Mashishimala Granite (Vearncombe et al., 1992). The zircons are subeuhedral, dark pink to red, inclusion free and compositionally zoned. U and Pb contents (Table 1) are low (99-348 and 28-97 ppm respectively). Four grains were analysed (Fig. 11) and yielded discordant results with an upper intercept age of 2820 ± 38 Ma (MSWD=0.0045). This age is interpreted as a minimum age for the emplacement of the Willie Granite. Consequently, the Willie Granite is older than the Mashishimala Suite and should be considered as a discrete intrusion.

Table 1 : U-Pb Data

Sample name	U ppm	Pb ppm	$^{206}Pb/^{204}Pb$	$^{206}Pb/^{238}U$	$^{207}Pb/^{235}U$	$^{207}Pb/^{206}Pb$	$^{207}Pb/^{206}Pb$ ages (Ma)
94-3							
ZrG3	35	20	631	0.4762	14.30	0.21775	2964±12
ZrG1	74	57	358	0.6184	18.73	0.21962	2978±15
ZrI1	65	48	268	0.6128	18.35	0.21723	2960±32
ZrH3	38	21	353	0.4433	13.25	0.21674	2957±15
ZrJ1	16	13	251	0.6914	20.80	0.21820	2967±33
94-6							
ZrK1	632	79	1786	0.1065	2.53	0.17217	2759±1
ZrG1	603	188	1796	0.2706	7.06	0.18911	2734±1
ZrJ1	652	92	1380	0.1238	3.27	0.19172	2757±1
ZrH1	435	147	879	0.3093	8.01	0.18789	2724±2
ZrI1	426	105	705	0.2233	5.61	0.18226	2674±2
ZrL1	576	122	2457	0.1800	4.64	0.18703	2716±2
ZrI2 (*)	151	37	283	0.2180	5.64	0.18778	2723±6
ZrJ2 (*)	178	41	677	0.2056	5.42	0.19127	2753±2
ZrK2 (*)	165	36	437	0.1962	4.96	0.18308	2681±4
ZrL2 (*)	151	44	470	0.2577	6.64	0.18674	2714±2
94-9							
ZrH1 p,t	28	22	456	0.6494	22.33	0.24935	3181±13
ZrI1 p,t	24	19	630	0.6201	20.90	0.24449	3149±11
ZrG1 p,t	55	37	268	0.5675	18.27	0.23347	3076±4
ZrK1 p,t	27	22	380	0.6671	22.87	0.24869	3176±19
ZrL1 p,t	20	16	431	0.6811	23.28	0.24789	3171±18
Zr JP p,m	1092	134	767	0.1128	3.77	0.24222	3135±9
ZrG2 p,t	65	52	524	0.6146	20.90	0.24669	3164±13
ZrH2 p,t	82	63	751	0.5951	20.15	0.24559	3157±10
Zr I2 p,m	467	149	613	0.2661	7.43	0.20259	2847±14
ZrJ2 p,m	202	118	673	0.4591	17.74	0.28023	3364±18
ZrL2 p,t	17	11	110	0.2827	9.69	0.24866	3176±10

(Table 1 continued)

94-12							
ZrG1	410	175	851	0.3689	10.63	0.20886	2897±10
ZrH1	189	64	798	0.2814	8.03	0.20691	2882±37
ZrDB1	293	91	531	0.2709	7.77	0.20801	2890±11
ZrDB2	283	328	432	0.3406	9.77	0.20807	2891±14
ZrB	60	9	153	0.1178	3.01	0.18522	2700±46
94-5							
ZrG1	197	100	461	0.4222	15.04	0.25838	3237±13
ZrJ1	449	91	532	0.1760	5.59	0.23055	3056±11
ZrK1	73	31	380	0.3543	12.31	0.25177	3196±14
W.F.							
ZrG (17)	55	43	208	0.6149	21.35	0.25185	3196±28
ZrQ (16)	50	41	584	0.6067	19.88	0.23769	3105±3
ZrRR (16)	78	61	402	0.6076	19.70	0.23520	3088±11
ZrEE (16)	181	131	822	0.5949	19.00	0.23168	3064±7
ZrFF (16)	35	28	413	0.6150	20.00	0.23584	3092±13
ZrNN (16)	89	72	327	0.6165	19.77	0.23259	3070±17
ZrE2 (16)	100	67	443	0.5057	16.52	0.23697	3100±12
ZrQ2 (16)	63	44	291	0.5723	18.53	0.23481	3085±27
ZrR2 (16)	56	36	592	0.5410	17.12	0.22947	3048±9
ZrF2 (16)	161	95	459	0.5009	16.90	0.24467	3151±13
ZrPP (16)	61	40	473	0.4911	15.92	0.23509	3087±13
ZrII (15)	279	66	247	0.1934	6.17	0.23160	3063±25
ZrKk (15)	157	47	104	0.2448	7.97	0.23617	3094±82
ZrJJ (15)	71	31	147	0.3701	11.73	0.22987	3051±54
Zr LL(15)	111	47	151	0.3204	8.92	0.20186	2841±48
94-8							
Zr GG	634	192	2673	0.2563	5.95	0.16851	2543 ± 4
Zr HH	160	87	747	0.4774	12.01	0.18249	2676 ± 8
Zr II	201	78	400	0.3437	8.34	0.17605	2616 ± 20
Zr KK2	254	65	530	0.2290	5.27	0.16696	2527 ± 13
Zr KK1	186	90	1053	0.4264	10.75	0.18282	2678 ± 7
Zr LL	167	82	440	0.4049	10.15	0.18181	2669 ± 18
94-11							
Zr AA	899	63	392	0.06654	0.5114	0.55743	442 ± 87
Zr BB	342	26	317	0.07444	0.5117	0.04985	188 ± 100
Zr DD	181	44	622	0.22785	5.5976	0.17817	2636 ± 19
Zr LL	79	53	507	0.57414	17.3028	0.21857	2970 ± 15
94-13							
Zr PP	151	66	808	0.38551	10.6892	0.20110	2835 ± 10
Zr QQ	114	73	318	0.54020	15.6846	0.21058	2910 ± 21
Zr RR	544	310	255	0.43708	13.0025	0.21575	2949 ± 12
Zr GG	1213	285	1611	0.21615	5.3148	0.17833	2637 ± 7
Zr HH	195	97	530	0.43537	12.7006	0.21157	2918 ± 18
Zr II	598	254	698	0.37516	11.0066	0.21278	2927 ± 13
Zr JJ	590	201	688	0.29446	8.2967	0.20435	2861 ± 9
Zr NN	171	97	585	0.49542	14.5754	0.21338	2921 ± 14
Zr EE	269	119	426	0.38167	10.7687	0.20463	2864 ± 14
Zr FF	622	182	529	0.25547	6.6492	0.18877	2731 ± 18
94-14							
ZrJJ (*)	300	80	597	0.24138	6.1277	0.18418	2690 ± 17
ZrKK (*)	154	30	307	0.16557	3.8692	0.17156	2573 ± 24
Zr K2 (*)	348	97	207	0.21898	5.4818	0.18155	2667 ± 22
ZrLL (*)	150	62	399	0.36661	9.8141	0.19415	2778 ± 10

(*) HF leached, m=metamict, p=pink, t=translucid

PYRITE

Pyrite fractions from seven samples, including the Malati Pump and Blue Jacket gold mines and the Gravelotte Emerald Mine, as well as accessory pyrite from a variety of host rocks, were analysed (Table 2). It is apparent that on the $^{207}Pb/^{204}Pb$ versus $^{206}Pb/^{204}Pb$ diagram (Fig. 12A) as well as the $^{208}Pb/^{204}Pb$ versus $^{206}Pb/^{204}Pb$ (Fig. 12B) diagram, pyrites exhibit a wide range of isotopic ratios, suggesting a multi-stage evolution for mineralization in the MGB.

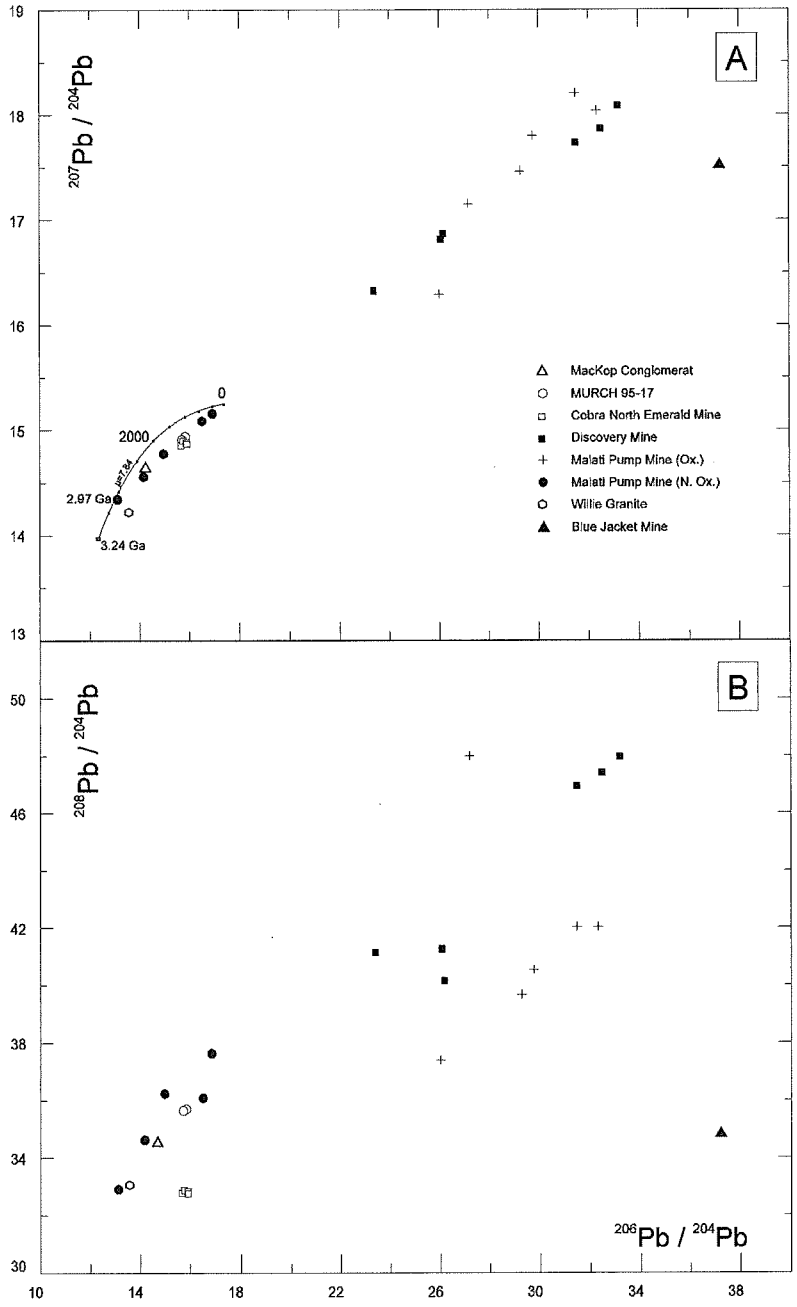

Figure 12 : $^{207}Pb/^{204}Pb$ versus $^{206}Pb/^{204}Pb$ and $^{208}Pb/^{204}Pb$ versus $^{206}Pb/^{204}Pb$ diagrams showing the results of analyses of pyrites from the Murchison terrain.

Table 2 : Pb-Pb Data

Sample Name	$^{208}Pb/^{204}Pb$	$^{207}Pb/^{204}Pb$	$^{206}Pb/^{204}Pb$	Pb ppm	U ppm
Discovery Emerald Mine					
Pyr 1 (*)	46.950	17.735	31.475	7	nd
Pyr 2 (*)	47.407	18.869	32.476	29	/
Pyr 3 (*)	47.970	18.085	33.176	/	/
Pyr 4 (#)	41.130	16.325	23.382	/	/
Pyr 5 (*)	41.260	16.810	26.053	/	/
Pyr 6 (*)	40.160	16.870	26.160	/	/
Malati Pump Mine (Au)					
Pyr 1 (*)	36.083	15.089	16.504	4,5	0.6
Pyr 2 (*)	32.905	14.346	13.117	/	/
Pyr 3 (#)	34.623	14.560	14.163	/	/
Pyr 4 (*)	36.238	14.776	14.961	9	/
Pyr 5 (*)	37.638	15.165	16.846	/	/
Pyr 6 ox.	42.037	18.203	31.462	16	1.4
Pyr 7ox.	39.671	17.463	29.263	5	/
Pyr 8 ox	37.390	16.291	26.004	9	/
Pyr 9 ox	42.031	18.039	32.323	16	/
Pyr 10 ox	40.527	17.800	29.752	4	/
Pyr 11 ox	47.992	17.150	27.162	/	/
Blue Jacket Mine (Au)					
Pyr 1 (#)	34.892	17.542	37.109	/	/
MURCH 95-17					
Pyr 2 (*)	35.707	14.944	15.833	/	/
Pyr 3 (#)	35.650	14.911	15.701	/	/
Mac Kop (MURCH 94-9)					
Pyr 1 (*)	34.600	14.900	14.870	/	/
Cobra North Emerald Mine					
Pyr 1 (*)	32.864	14.899	15.741	33	0.06
Pyr 2 (*)	32.818	14.880	15.874	/	/
Pyr 3 (*)	32.778	14.856	15.660	18	/
Pyr 4 (*)	32.761	14.870	15.892	/	/
Willie Granite (MURCH 94-14)					
Pyr 1 (#)	33.113	14.233	13.312	/	/

(*) : Euhedral pyrites, (#) : Pyrite of uncertain origin

Mineralization along the Antimony Line

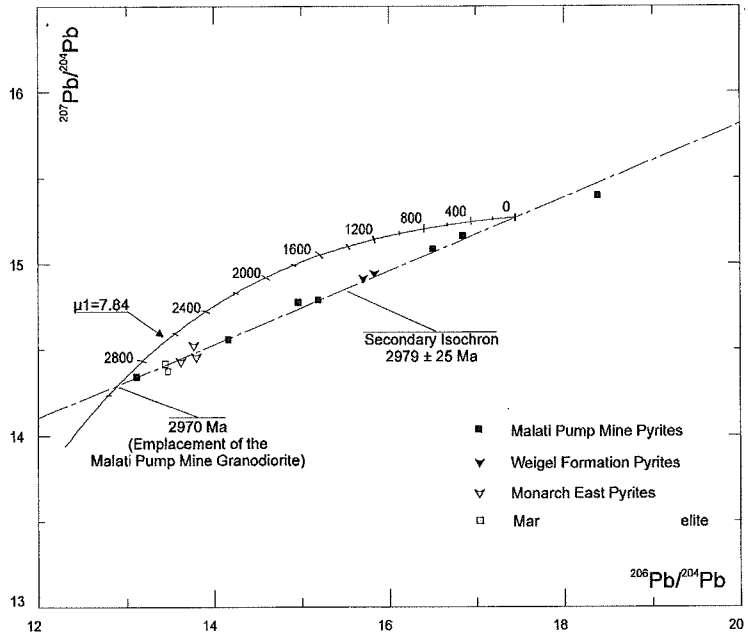

Figure 13 : $^{207}Pb/^{204}Pb$ versus $^{206}Pb/^{204}Pb$ diagram showing the results for pyrites from the Malati Pump Mine.

Pyrite extracted from the Malati Pump Mine granodiorite are divided in two types, namely, unaltered and oxidized pyrites. The latter show an intense reddish colour (limonite or goethite) which is characteristic of pyrite that has been preferentially leached of its sulphur by an oxidizing fluid.

The U and Pb contents are 600 ppb and 4.5-9 ppm respectively, for the unaltered type, and 1.2 ppm and 4-16 ppm respectively for the oxidized variety (Table 2). On the $^{206}Pb/^{204}Pb$-$^{207}Pb/^{204}Pb$ diagram (Fig. 13) the fresh pyrites plot together with Vearncombe's data (1992), as well as pyrite from the felsic schist of the Weigel Formation. This data collectively define a Pb-Pb isochron (MSWD=6) which yields an age of 2979 ± 25 Ma with μ1=7.84. It is interesting to note that the pyrites from the Monarch East Mine (Saager and Koppel, 1976) also plot close to this isochron. In addition, two sphalerite samples from the Maranda deposit, a presently active Cu-Zn mine in the Rubbervale Formation, also have Pb isotopic ratios that fall on the isochron. The oxidized pyrites from the Malati Pump deposit on the Antimony Line display more radiogenic $^{206}Pb/^{204}Pb$ and $^{207}Pb/^{204}Pb$ ratios than the unaltered grains, but the data are more scattered and do not yield any age information (Fig. 14).

Discovery Gold Mine and Gravelotte Emerald Mine

The lead isotopic compositions of the Discovery Gold Mine pyrite are more radiogenic than grains from the Cobra North emerald pit which display a restricted range of values. For both sets of pyrites the Pb concentrations vary from 7 to 33 ppm (Table 2). On a $^{207}Pb/^{204}Pb$ versus $^{206}Pb/^{204}Pb$ diagram (Fig. 14), a regression line through the data from the present study, together with that from Vearncombe et al. (1992) for Cobra North, define an age of 2690 ± 35 Ma (MSWD=1120) and an apparent first stage μ1=6.69 (starting from 3.24 Ga). A high MSWD and a low μ1 value indicate that the age of 2690 Ma has no geological meaning.

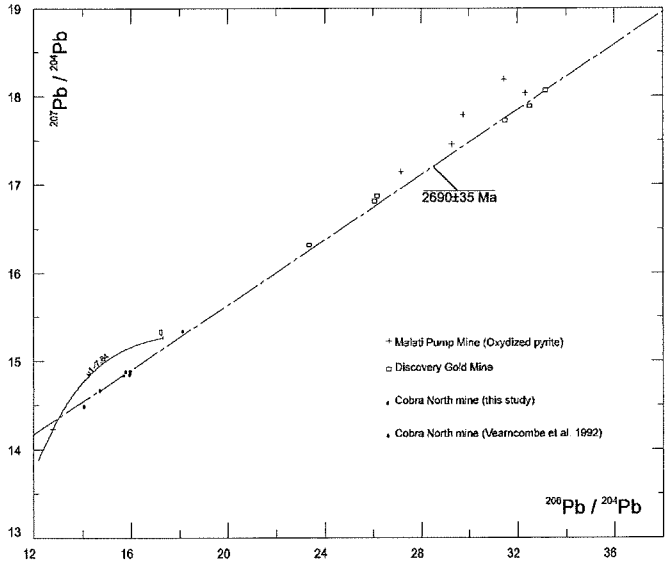

Figure 14 : $^{207}Pb/^{204}Pb$ versus $^{206}Pb/^{204}Pb$ diagram showing the results for pyrites from the Discovery and Cobra North Mine.

DISCUSSION

The age data indicate that felsic volcanism and sedimentation in the northern and eastern portions of the MGB occurred between 3.09 and 2.97 Ga. The upper limit is provided by the age of the Rubbervale Formation. The lower limit is constrained by the maximum ages of the Weigel and the Mac Kop formations and is also based on the assumption that sedimentation and volcanism in the south and central portions of the MGB were coeval. The MGB is, therefore, significantly younger than the BGB and deposition of the greenstone belt appears to have been accomplished in a fairly short span of time.

Implications for Kaapvaal crustal evolution and metallogeny

Although previously considered similar to the 3.45 - 3.25 Ga BGB, the MGB is now shown to have been deposited over a relatively restricted period between 3.09 - 2.97 Ga. The BGB and environs records 800 Ma of crustal history; the volcano-sedimentary sequence and associated TTG gneisses were deposited episodically at around 3.45 Ma and 3.23 Ga (Kamo and Davis, 1994); emplacement of major K-rich batholiths occurred at 3.105 Ga and sporadic granitoid plutonism took place at 2.9 Ga and 2.7 Ga (Meyer et al., 1994). Mesothermal gold-lode deposits in the BGB formed along major compressional and strike-slip shears at around 3.1 Ga (Harris et al., 1995).

By contrast with the extended record of crustal evolution preserved in the Barberton region, the MGB formed over a much shorter period of time, when there was little or no magmatic activity recorded in the latter area. The tectonic evolution of the MGB is linked to compressional events associated with the onset of the Limpopo Orogeny to the north. The southern extent of strain related to the orogeny is believed to be manifest along an extensive zone of strike-slip and southward-directed shearing on the northern edge of the MGB, which now forms part of the Thabazimbi-Murchison Lineament (McCourt, 1995).

De Wit et al. (1992) have suggested that the northeastern Kaapvaal Craton was assembled between 2.9 -2.7 Ga from a collage of at least 5 terranes, of which the Murchison and the Pietersburg-Sutherland greenstone belts formed two discrete domains. The Pietersburg belt (Fig. 1) consists, in part, of a sequence of syntectonic, thrust-related, coarse clastic rocks (the Uitkyk Formation) which has been bracketed by single zircon dating at between 2.9 and 2.7 Ga, and is, therefore, a time equivalent of the upper portion of the Witwatersrand Supergroup (De Wit et al., 1993). The mafic and ultramafic volcanics which underlie these sediments are thought to be similiar in age to the Barberton sequences although there is no reliable age data to confirm this and they may be younger. It is, however, apparent that both the Murchison and Pietersburg- Sutherland greenstone belts are aligned along, and form part of, the Thabazimbi-Murchison Lineament. The latter, in all likelihood, represents the locus of volcano-sedimentary accumulations along the northern extent of the Kaapvaal continent at that time.

The MGB has been interpreted as part of an exhumed island arc developed along the northern edge of the Kaapvaal continent (Vearncombe et al., 1992 ; McCourt, 1995), and possibly accreted to the continent along the TML at some time prior to the Limpopo Orogeny. Support for the island arc hypothesis was provided by the putative link between the Rooiwater Complex and the Rubbervale Formation and the suggestion that the former represents the subvolcanic chamber beneath chemically related extrusive calc-alkaline volcanics. Such a link is no longer feasible in terms of the present data and the Rooiwater Complex must now be regarded as a 2.74 Ga mafic intrusion which has been dismembered from the lower part of its cumulate and tectonically emplaced into its present subvertical position along a major Limpopo-related décollement.

Granite magmatism in and around the Murchison greenstone belt

The MGB was deposited over a relatively short period of time between 3.09 and 2.97 Ga either as a magmatic arc accreted to the edge of an existing >3.1 Ga continent, or as a rift-related

sequence within it (Poujol et al., 1996). At least three periods of granite magmatism have now clearly been identified as associated with the formation of the MGB, or post-dating it:-

1. The Malati Pump Mine and Discovery Mine granites were emplaced at 2970 ± 15 Ma and 2960 ± 43 Ma respectively. The Maranda Granodiorite, which outcrops at the western extremity of the Antimony Line, has also yielded an age of 2901 ± 20Ma, which is considered to be a minimum estimate for the emplacement of this body . In the light of these results, we suggest that all 3 intrusions were emplaced at ca. 2.97 Ga and, therefore, represent components of a major batholith in this region. The Antimony Line probably represents the locus along which this batholith was emplaced, confirming the suggestion by De Beer et al. (1984) that this structural feature has been intruded by granite along it entire extent. In addition the age obtained for the felsic volcanics of the Rubbervale Formation indicate that this unit must represent the extrusive equivalent of the plutonic rocks described above. We refer to this suite, which comprises both the granites and Rubbervale Formation, as the Maranda batholith and suggest that a major period of felsic magmatism took place at 2.97 Ga.

2. There is a suggestion that granitoid emplacement also occured at 2.82 Ga, which is the age provided by the Willie Granite which outcrops along the southern flank of MGB. Although there is no other evidence of granitoid emplacement at this time in the MGB, this age is similar to those obtained for syntectonic granitoids linked to horizontal shortening across the Pietersburg Greenstone Belt at ca 2.8 Ga (De Wit et al., 1993). It is also relevant to note that several other granites, such as the Mooihoek, Mhlosheni, Spekboom and Godlwayo S-type plutons in Swaziland (Meyer et al., 1994), and the Schweizer-Reneke batholith in the western part of the Craton (Robb et al., 1992) all yield ages of 2.82 - 2.88 Ga, suggesting that this was a major period of felsic magmatism on the Kaapvaal Craton.

3. The Mashishimala Granite yielded an age of 2677 ± 14 Ma which reflects the age of one of the early compressional events associated with Limpopo orogenesis (Barton, 1992). Many of the late-stage, potassic granite plutons of the Kaapvaal Craton also yield ages of ca. 2700 Ma, indicating that this period was also an important crust-forming event in the MGB region and elsewhere.

Mineralization processes

Previous work

In an early study of the isotopic characteristics of mineralization in MGB, Saager and Koppel (1976) measured very low, non-radiogenic, Pb-isotopic ratios for galenas from the Old Star Gold Mine along an extension of the Antimony Line. These data yielded a model ages of 3.25 Ga for the sulphides and constrained the maximum age of mineralization at ca. 3.02 Ga. Vearncombe et al. (1992) performed Pb-Pb analyses on a number of samples representing all the various styles of mineralization in the MBG. Sulphides from Letaba and Ngwabu on the Cu-Zn line and from the Eldorado, Novengilla and Old Star gold mines define a secondary isochron with an age of ca. 3.1 Ga, with a Pb source at approximately 3.25 Ga. Other sulphide separates from the Gravelotte Emerald Mine and the Malati Pump gold deposit also defined a secondary isochron with an age of ca. 2.85 Ga. These authors concluded that mineralization in the MGB was episodic and formed between 3.25 and 2.8 Ga.

Present study

The Pb-Pb isotopic data for sulphide minerals in the MGB from both previous work (Saager and Koppel, 1976; Vearncombe et al., 1992) as well as the present study, indicate that some of the

data define a well constrained secondary isochron whose age (i.e. 2979 ± 25 Ma) is consistent with that for the Maranda batholith and Rubbervale Formation. Other data, however, shows considerable scatter with no meaningful age significance, and plots below the 2979 Ma secondary isochron.

In the $^{207}Pb/^{204}Pb$ versus $^{206}Pb/^{204}Pb$ plot of Figure 13, the 2979 Ma secondary isochron is shown to intersect a model Pb isotopic growth curve calculated for a μ of 7.84. The secondary isochron intersects the growth curve at 2970 Ma, indicating that mineralization in the MGB is related to the Maranda batholith-Rubbervale Formation emplacement and that the Pb is also derived from this source. This contradicts previous workers who suggested that mineralization was episodic and derived from an older basement source.

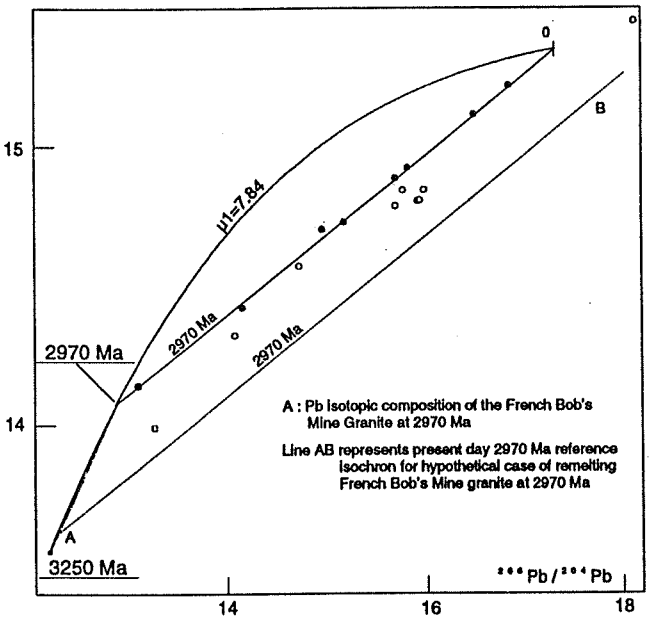

Figure 15: Pb-Pb diagram showing the mixing model

The remaining data, which scatters over a wide array below the secondary isochron is best explained in terms of a mixing model. In the $^{207}Pb/^{204}Pb$ versus $^{206}Pb/^{204}Pb$ plot of Figure 15 the MGB data from the present study is subdivided along geographic lines into points derived from well within the belt (solid symbols), and those derived from along the southern margin of the belt (open symbols). This subdivision coincides exactly with those points that fall on the secondary isochron (solid symbols) and those that fall below this reference (open symbols). It is known that the southern margin of the MGB is flanked by an older gneissic basement represented by the French Bob granite, whose age is 3228 ± 12. If a hypothetical line is plotted which represents a 2970 Ma reference isochron for French Bob granite re-homogenized at that time (line AB; Figure 15), a lower limit for all the Pb isotopic ratios obtained from mineralized areas along the southern portion of the belt is obtained. It is , therefore, suggested that these isotopic ratios could be the result of mixing between Pb derived from the older gneissic basement and that characteristic of the major magmatic event at 2.97 Ga. Pb isotopic ratios from well within the greenstone belt (i.e the Antimony Line and its Sb-Au mineralization and the base metal mineralization of the Cu-Zn line), appear to be uncontaminated with respect to the older basement and to represent a single mineralizing event where the metals were derived from the magma itself.

MGB as a type-source for Witwatersrand gold

Recent single grain U-Pb zircon dating has constrained sedimentation in the Witwatersrand Basin (Fig. 1, inset) to between 3.074 and 2.714 Ga (Armstrong et al., 1991). The lower West Rand Group (WRG) was deposited between 2,970 - 2,914 Ma, whereas the upper, auriferous Central Rand Group (CRG) was laid down between 2,894 - 2,714 Ma (Robb et al., 1991). It is widely held that at least some of the gold in the CRG was introduced as micronuggets with a major proportion representing authigenic gold remobilized during post-depositional processes (Robb and Meyer, 1991) and/or added by hydrothermal solutions (Phillips and Myers, 1989).

The ages of detrital zircon and monazite grains provide a good indication of the age range of

source material during Witwatersrand sedimentation. The histogram of ages (Fig. 16) for detritus in the Witwatersrand Supergroup relative to the age brackets for the MGB demonstrates that much of the material that was being supplied into the WRG was older than the MGB. Nevertheless, a substantial proportion of sediment deposited into the CRG came from material similiar in age, or younger, than the Murchison Greenstone Belt.

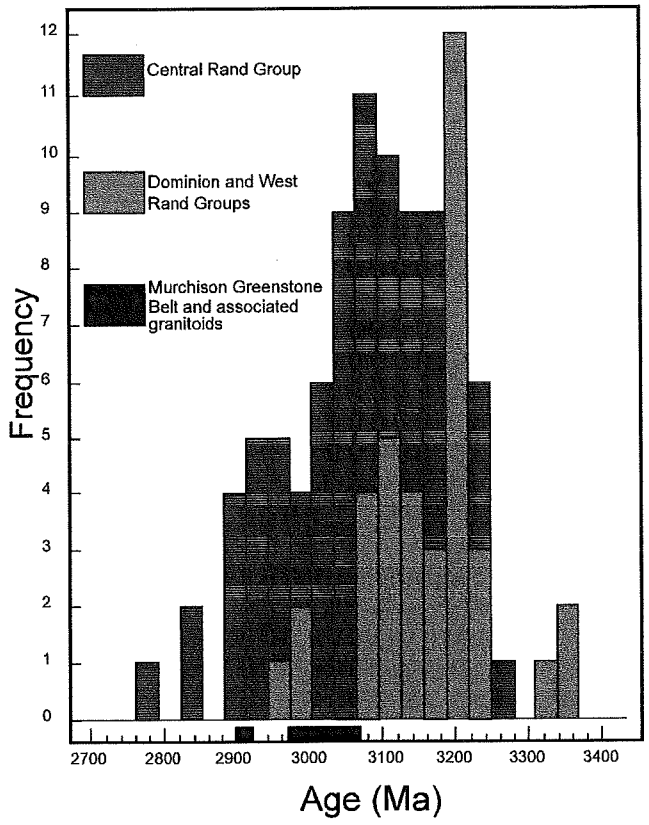

Figure 16 : Histogram showing the distribution of detrital zircon and monazite ages

The above data, therefore, support Vearncombe's (1992) contention that the MGB, as well as other volcano-sedimentary sequences that might have developed along the TML, represent a viable source for Witwatersrand gold. The Kraaipan and Amalia greenstone belts that occur along the western edge of the Kaapvaal Craton, possibly represent time equivalents and distal analogs of the MGB. They are known to contain significant, albeit small, banded iron formation hosted lode gold-deposits. The high-level (epithermal?) epigenetic Sb-As-Au-Hg mineralization associated with the Antimony Line in the MGB possibly represents one of the deposit types that might have supplied detrital gold into the Witwatersrand Basin. These deposits have been cited as an explanation for the very high mercury contents that typify Witwatersrand gold particles (Von Gehlen, 1983). These deposits have also been cited as an explanation for the very high mercury contents that typify Witwatersrand gold particles (Von Gehlen, 1983), although some workers prefer to view this feature as an indication of in-situ gold remobilization (Frimmel et al., 1993). Vearncombe's model previously lacked the support of a well-constrained chronological framework, but the availability of accurate age constraints for the MGB, as well as the age distribution pattern of Witwatersrand detritus, now effectively removes this encumbrance to the model and the data reported here strongly support the contention that the MGB and its equivalents along the TML may played an important role as a source for Witwatersrand detritus.

CONCLUSIONS

The Murchison greenstone belt has now been shown to be considerably younger than the 3.4 to 3.2 Ga Barberton greenstone belt some 200 km to its south. Single zircon U-Pb age determinations on metavolcanics in the MGB yield ages of 3087 Ma and 2971 Ma, while the youngest detrital zircons in metaconglomerate from within the belt are 3076 Ma. The volcano-sedimentary sequence has, therefore, been deposited between ca. 3.09 and 2.97 Ga. The oldest granites recognized thus far in the region are the tonalitic-trondhjemitic gneisses along the southern margin of the MGB, dated at 3228 Ma. The Maranda batholith, which intrudes the central portion of the belt along the Antimony Line, was emplaced at 2.97 Ga and appears to represent the plutonic equivalent of the acid extrusive rocks comprising the Rubbervale Formation, which is also 2.97 Ga old. Younger granite events in the region are represented by the 2.82 Ga Willie granite and the 2.67 Ga Mashishimala granite, both to the south of the belt. It has been suggested that the MGB represents the remnants of a magmatic arc that was accreted onto the northern margin of a continent that had substantially formed by 3.1 Ga (Vearncombe, 1992; Poujol et al., 1996), but the details of

how this occurred are still uncertain.

The Murchison region contains the world's largest antimony mine and has world class reserves of both antimony and gold in several deposits along the 35km long Antimony Line. This mineralization is hydrothermal in character and structurally controlled, and forms part of an unusual Mo-W-Be-Sb-Au-B-Hg paragenesis which has recently been attributed to fluid egress from a granitic source (Kedda et al., 1990). Strong support for this notion is derived from the present study in which pyrite from the Malati Pump and Monarch East deposits define a secondary Pb-Pb isochron whose age is ca. 2.97 Ga, essentially indistinguishable from the emplacement age for the Maranda batholith which has intruded the Antimony Line. This structural feature, which must have been present prior to the emplacement of the 2.97 Ga felsic magmas, not only represents the locus for intrusion of the batholith, but also focussed fluids that, at least initially, appear to have been derived from the volatile saturated granite.

The major emerald deposits that occur along the southern margin of the MGB, which are also associated with numerous small gold (± Mo,Sb?) deposits, contain pyrites that typically plot below the 2.97 Ga secondary isochron discussed above. These Pb isotopic signatures are interpreted to reflect a mixing of Pb from an older, 3.23 Ga continental source and from the 2.97 Ga Maranda batholith. It is, therefore, suggested that it is unnecessary to invoke episodic stages of mineralization, as suggested by Vearncombe et al. (1992) since all the mineralization in the region can be related to the 2.97 Ga event, with variable degrees of mixing to account for those samples which do not fall on the isochron. It would appear at this stage that mineralization that has formed along the margins of the belt have incorporated a component of older continent, whereas ore deposits within the MGB have undergone little or no mixing. The interpretation that emeralds represent porphyroclasts formed during an event of regional metamorphism (Grundmann and Morteani, 1989) implies that the metamorphic overprint must have been coeval with the emplacement of the Maranda batholith, and not a significantly later event. Emerald formation, and specifically the source of beryllium, would appear to be intimately associated with granite emplacement and not simply the result of metamorphic mineral reactions.

It is also interesting to note that the Pb isotopic ratios of two sphalerite samples from the Maranda Cu-Zn deposit in the Rubbervale Formation (from Vearncombe et al., 1992) also plot on the 2.97 Ga secondary isochron defined by sulphides from the Antimony Line. This suggests that base metal mineralization in the MGB formed at the same time as the emplacement of the Rubbervale Formation at 2.97 Ga, supporting studies that describe this style of mineralization as a syngenetic, VMS style (Taylor, 1981; Terblanche and Lewis, 1995). Further studies on the origin and isotopic characteristics of this mineralization are currently underway (Poujol in prep.).

In summary, the Maranda batholith and its extrusive component, the Rubbervale Formation, appears, therefore, to be genetically linked to all the main styles of mineralization in the MGB. Gold and emerald mineralization is spatially associated the granite that was itself intruded into structures that also controlled subsequent magmatic fluid egress into high levels of the crust. Volcanogenic base metal sulphide mineralization is associated with the extrusive component of the 2.97 Ga felsic magmatic event and may have involved circulation of surface fluids. The Maranda batholith and Rubbervale Formation apparently represents a highly prospective metallotect that has implications, not only for exploration in the Murchison region itself, but for the important question of the source of Witwatersrand gold, for which a causative link has already been made (Vearncombe, 1992; Poujol et al., 1996). Older continental crust was in existence, particularly to the south of the present position of the belt, and has contributed to the ore-forming components, but isotope systematics within the MGB suggest that much of the belt represents juvenile addition of crust. Major

deformation within the MGB took place between 3.09 and 2.97 Ga although subsequent compression also affected the belt during Limpopo orogenesis at ca. 2.7 Ga.

REFERENCES

Anhaeusser, C.R., Wilson, J.F. (1981) The granite-gneiss greenstone shield. In: Hunter, D.R: (ed.) Precambrian of the Southern hemisphere. Elsevier Scientific Publishing Company, Amsterdam Oxford New York, pp. 423-442

Armstrong, R.A., Compston, W., de Wit, M.J., Williams, I.S. (1990) The stratigraphy of the 3.5-3.2 Barberton greenstone belt revisited : a single zircon ion microprobe study. Earth Planet. Sci. Lett. 101: pp. 90-106

Armstrong, R.A., Compston, W., Retief, E.A., Williams, I.S. and Welke, H.J., 1991, Zircon ion-microprobe studiesbearing on the age and evolution of the Witwatersrand Triad: Precambrian Research, v. 53, p. 243-266.

Barton, J.M., Allsopp, H. (1984) Pb-Isotopic evidence of the timing and mechanisms of mineralization in the Barberton granite-greenstone terrane. Barberton Centenary Symposium, Barberton, South Africa. Abstracts and Guidebook, pp. 4

Barton, E.S., Compston, W., Williams, I.S., Bristow, J.W., Hallbauer, D.K. and Smith, C.B., 1989, Provenanceages for the Witwatersrand Supergroup and the Ventersdorp Contact Reef: constraints from ion-microprobe U-Pb ages of detrital zircons: Economic Geology, v. 84, p. 2012-2019.

Brandt, G. and Kröner, A., 1993, Preliminary results of single zircon studies from various archaean rocks of the NETransvaal. 16th Colloqium of African Geology, Mbabane, p. 54-56.

Brandl, G. ,Jaeckel, P., Kröner, A. (1996) Single zircon age for the felsic Rubbervale Formation, Murchison Greenstone Belt, South Africa. S.Afr.J.Geol. 99, pp. 229-234

Bruguier, O., Dada, S., Lancelot, J.R. (1994) Early Archaean component (>3.5 Ga) within a 3.05 Ga orthogneiss from northen Nigeria : U-Pb zircon evidence. Earth Planet. Sci. Lett. 125, pp. 89-103

De Beer, J.H. (1982) A geophysical study of the Murchison greenstone belt, South Africa. Rev. Bras. Geosc. 12, pp. 105-112

De Beer, J.H., Stettler, E.H., Duvenhage, A.W.A., Joubert, S.J., Raath, C.J. (1984) Gravity and geoelectrical studies of the Murchison Greenstone belt, South Africa. Trans. Geol. Soc. S. Afr. 87, pp. 347-359

De Ronde, C.E.J., Kamo, S.L., Davis, D.W., De Wit, M.J. and Spooner, E.T.C., 1991, Field, geochemical and U-Pb isotopic constraints from hypabyssal felsic intrusions within the Barberton greenstone belt, South Africa; Implications for tectonics and timing of gold mineralization. Precambrian Research, 49, p. 261-280.

De Wit, M.J., Roering, C., Hart, R.J., Armstrong, R.A., de Ronde, C.E.J., Green, R.W.E., Tredoux, M., Peberdy, E. and Hart, R.A., 1992, Formation of an Archaean continent: Nature, v. 357, p. 553-562.

De Wit, M.J., Armstrong, R.A., Kamo, S.L. and Erlank, A.J., 1993, Gold-bearing sediments in the Pietersburg greenstone belt: age equivalents to the Witwatersrand Supergroup sediments, South Africa: Economic Geology, v.88, p. 1242-1252.

Frimmel, H.E., Le Roex, A.P., Knight, J. and Minter, W.E.L., 1993, A case study of the postdepositional alteration of the Witwatersrand Basal Reef gold placer: Economic Geology, v.88, p. 249-265.

Grundmann, G. And Morteani, G. (1989) Emerald mineralization during regional meatmorphism: The Habachtal (Austria) and Leydsdorp (Transvaal, South Africa) deposits. Econ. Geol. 84, pp. 1835-1849.

Hall, A.L. (1912) The Geology of Murchison Range and District. Mem. Geol. Surv. S. Afr. 6, 184 pp

Hausmann, S.G. (1959) A mineralogical investigation of the Letaba copper-zinc ores and the Monnarch Cinnabar deposits located in the Murchison Range of the Eastern Transvaal. Unpubl. M.Sc. Thesis, Univ. of the Witwatersrand, Johannesburg

Harris, P.D., Robb, L.J. and Tomkinson, M.G., 1995, The nature and structural setting of rare-element pegmatite along the northern flank of the Barberton greenstone belt, South Africa: South African Journal of Geology, v.98, p. 82-94.

Kamo, S.L., Davis, D.W. (1994) Reassement of Archaean crustal development in the Barberton Moutain Land, South Africa, based on U-Pb dating. Tectonics 13, pp. 167-192

Kedda, S.W. (1992) Geochemical and stable isotope studies of gold bearing granitoids in the Murchison Schist Belt, North Eastern Transvaal. Unpubl. M.Sc. Thesis, Univ. of the Witwatersrand, Johannesburg

Kedda, S.W., Robb, L.J., Meyer, F.M., Verhagen, B.Th (1990) Gold mineralization associated with albitized felsic intrusions in the Murchison greenstone belt, South Africa. Third International Archaean Symposium, Perth, Australia

Krogh, T.E. (1982) Improved accuracy of U-Pb ages by the creation of more concordant systems using an air abrasion technique, Geochim. Cosmochim. Acta 46, pp. 617-649

Lancelot, J., Vitrac, A., Allegre, C.J. (1976) Uranium and lead isotopic dating with grain by grain zircon analysis : A study of complex geological history with a single rock, Earth Planet. Sci. Lett. 29, pp. 357-366

Ludwig, K.R. (1993a) A Computer Program for Processing Pb-U-Th Isotope Data. US Geol. Survey, Open File Rep. 88-542, 32 pp.

Ludwig, K.R. (1993b) A plotting and regression program for radiogenic-isotope data. US Geol. Survey, Open File Rep. 91-445, 42 pp.

McCourt, S., 1995 , The crustal architecture of the Kaapvaal crustal block, South Africa, between 3.5 and 2.0 Ga: Mineralium Deposita, v.30, p. 89-97.

Meyer, F.M., Robb, L.J., Reimold, W.U. and De Bruiyn, H., 1994, Contrasting low- and high-Ca granites in the Barberton Mountain Land, Southern Africa: Lithos, v.32, p. 63-76.

Minnitt, R.C.A. (1981) The regional geological setting of the Murchison Range with particular reference to the copper-zinc line. Int. Rep., Anglovaal Ltd

Minnitt, R.C.A., Anhaeusser, C.R. (1992) Gravitational and diapiric structural history of the eastern portion of the Archaean Murchison Greenstone Belt, South Africa. J. Afr. Earth Sci. 15, pp. 429-

440

Phillips, G. N. and Myers, R.E., 1989, The Witwatersrand gold fields : Part II. An origin for Witwatersrand gold during metamorphism and associated alteration : Economic. Geology MON. 6, p. 598-608.

Pearton, T.N.(1986) The Monarch Cinnabar Mine : Murchison Greenstone Belt. In: Anhaeusser, C.R., Maske, S. (ed.) Mineral Deposits of Southern Africa. Geol. Soc.S. Af., Johannesburg, pp. 339-348

Pearton, T.N., Viljoen, M.J. (1986) Antimony mineralization in the Murchison Grenstone Belt:: An overview. In: Anhaeusser, C.R., Maske, S. (ed.) Mineral Deposits of Southern Africa. Geol. Soc.S. Af., Johannesburg, pp. 293-320

Poujol, M., Respaut, J.P., Robb, L.J., Anhaeusser, C.R. and Lancelot, J.R., 1995, The Archaean Murchison Schist Belt, Kaapvaal craton, South Africa in the light of new U-Pb data: Terra Abstracts, v. 7, p. 353-354.

Poujol, M., Robb, L.J., Respaut, J.P., Anhaeusser, C.R. (1996) 3.07-2.97 Ga Grenstone Belt formation in the northeastern Kaapvaal Craton : Implications for the origin of the Witwatersrand Basin, Econ. Geol. 91, pp. 1455-1461.

Reynolds, I.M. (1986) Vanadium-bearing titaniferous iron ores of the RooVwater Complex, North-Eastern Transvaal. In: Anhaeusser, C.R., Maske, S. (ed.) Mineral Deposits of Southern Africa. Geol. Soc.S. Af., Johannesburg, pp. 451-460

Robb, L.J., Robb, V.M. (1985) Archaean pegmatite deposits in the North-Eastern Transvaal. In: Anhaeusser, C.R., Maske, S. (ed.) Mineral Deposits of Southern Africa. Geol. Soc.S. Af., Johannesburg, pp. 437-449

Robb, L.J., Davis, D.W. and Kamo, S.L., 1990, U-Pb ages on single detrital zircon grains from the Witwatersrand basin, South Africa: constraints on the age of sedimentation and on the evolution of granites adjacent to the basin: Journal of Geology, v. 98, p. 311-328.

Robb, L.J., Davis, D.W. and Kamo, S.L., 1991, Chronological framework for the Witwatersrand Basin and environs : towards a time constrained depositional model: South African Journal of Geology, v. 94, p. 86-95.

Robb, L.J. and Meyer, F.M., 1991, A contribution to recent debate concerning epigenetic versus syngenetic mineralization processes in the Witwatersrand Basin: Economic Geology, v. 86, p. 396-401.

S.A.C.S. (1980) The Murchison Sequence. In: Kent L.E. (ed.) Stratigraphy of South Africa, Part 1. Lithostratigraphy of the Republic of South Africa, South West Africa/Namibia and the Republics of Bophuthatswana, Transkei and Venda, Handbook Geol. Surv. S. Afr., pp. 45-52

Saager, R. (1973) Metallogenese präkambrischer Goldvorkommen in den vulkano-sedimentären Gesteinskomplexen (greenstone belts) der Swaziland Sequenz in Südafrika. Geol. Rundschau 62, pp. 888-901

Saager, R. (1974) Geologische und geochemische Untersuchungen and primären und sekundären Goldvorkemmen im frühen Präkambriun Südafrikas : Ein Beitrag zur Deutung der primären Herkunft des Goldes in der Witwatersrand Lagerstätte. Unpubl. Habilitation Thesis, Univ. Heidelberg

Saager R., Koppel, V. (1976) Lead isotopes and trace elements from sulfides of Archaean greenstone belts in South Africa - a contribution to the knowledge of the oldest know mineralizations. Econ. Geol. 71, pp. 44-57

Terblanche, H.K. and Lewis, R.D. (1995) An overview of the Maranda basemetal mine. Centennial Geocongress, Geol. Soc. S. Afr., Johannesburg, Ext. Abst. Vol. 1, pp 111-114.

Treloar, P.J., Coward, M.P., Harris, N.B.W. (1992) Himalayan-Tibetan analogies for the evolution of the Zimbabwe Craton and Limpopo Belt. Prec. Research 55, pp. 571-587

Van Eeden, O.R., Partridge, F.C., Kent, L.R., Brandt, J.W. (1939) The mineral deposit of the Murchison Range east of Leydsdorp. Mem. Geol. Surv. S. Afr. 36, 172 pp.

Vearncombe, J.R. (1992) The Murchison belt, Kaapvaal Craton : A possible source for Witwatersrand Gold ? In: Glover, J.E., Ho, S.E. (ed.), Third International Archaean Symposium, Perth, 22, pp. 409-422

Vearncombe, J.R., Cheshire, P.E., De beer, J.H., Killick, A.M., Mallinson, W.S., McCourt, S., Stettler, E.H. (1988) Structures related to the Antimony Line, Murchison Schist Belt, Kaapvaal Craton, South Africa, Tectonophysics 154, pp. 285-308

Vearncombe, J.R., Barton, J.M., Cheshire, P.E., De Beer, J.H., Stettler, E.H., Brandl, G. (1992) Geology, geophysics and mineralization of the Murchison Schist Belt, Rooiwater Complex and surrounding granitoids. Mem. Geol. Surv. S. Afr. 81, 139 pp

Viljoen, M.J., Van Vuuren, C.J.J., Pearton, T.N., Minnit, R.C.A., Muff, R., Cilliers, P. (1978) The regional geological setting of mineralization in the Murchison range with particular reference to antimony. In: Verwoerd, W.J. (ed.) Mineralization in metamorphics terranes. Geol. Soc. S. Afr., pp. 55-86

Viljoen, R.P., Saager, R., Viljoen, M.J. (1969) Metallogenesis and ore control in the Steynsdorp Goldfield, Barberton Moutain Land, South Africa. Econ. Geol. 64, p. 778-797

Viljoen, R.P., Saager, R., Viljoen, M.J. (1970) Some thoughts on the origin and processes responsible for the concentration of gold in early Precambrian of southern Africa, Mineral. Deposita 5, pp. 164-180

Von Gehlen, K., 1983, Silver and mercury in single gold grains from the Witwatersrand and Barberton, South Africa. Mineralium Deposita, v. 18, p. 529-534.

____oOo____